

This article was downloaded by:

On: 25 January 2011

Access details: *Access Details: Free Access*

Publisher *Taylor & Francis*

Informa Ltd Registered in England and Wales Registered Number: 1072954 Registered office: Mortimer House, 37-41 Mortimer Street, London W1T 3JH, UK



## Separation Science and Technology

Publication details, including instructions for authors and subscription information:

<http://www.informaworld.com/smpp/title~content=t713708471>

### Simultaneous Absorption of H<sub>2</sub>S and Co<sub>2</sub> Into Aqueous Methyldiethanolamine

Noman Hamour<sup>a</sup>; Ali Bidarian<sup>a</sup>; Orville C. Sandall<sup>a</sup>

<sup>a</sup> Department of Chemical and Nuclear Engineering, University of California, Santa Barbara, California

**To cite this Article** Hamour, Noman , Bidarian, Ali and Sandall, Orville C.(1987) 'Simultaneous Absorption of H<sub>2</sub>S and Co<sub>2</sub> Into Aqueous Methyldiethanolamine', *Separation Science and Technology*, 22: 2, 921 – 947

**To link to this Article:** DOI: 10.1080/01496398708068990

URL: <http://dx.doi.org/10.1080/01496398708068990>

## PLEASE SCROLL DOWN FOR ARTICLE

Full terms and conditions of use: <http://www.informaworld.com/terms-and-conditions-of-access.pdf>

This article may be used for research, teaching and private study purposes. Any substantial or systematic reproduction, re-distribution, re-selling, loan or sub-licensing, systematic supply or distribution in any form to anyone is expressly forbidden.

The publisher does not give any warranty express or implied or make any representation that the contents will be complete or accurate or up to date. The accuracy of any instructions, formulae and drug doses should be independently verified with primary sources. The publisher shall not be liable for any loss, actions, claims, proceedings, demand or costs or damages whatsoever or howsoever caused arising directly or indirectly in connection with or arising out of the use of this material.

## Simultaneous Absorption of H<sub>2</sub>S and CO<sub>2</sub> Into Aqueous Methyldiethanolamine

NOMAN HAIMOUR, ALI BIDARIAN, and ORVILLE C. SANDALL

DEPARTMENT OF CHEMICAL AND NUCLEAR ENGINEERING  
UNIVERSITY OF CALIFORNIA  
SANTA BARBARA, CALIFORNIA 93106

### ABSTRACT

The tertiary amine methyldiethanolamine (MDEA) is finding increasing application as a chemical solvent for selective absorption of hydrogen sulfide from gases containing hydrogen sulfide and carbon dioxide. Gas streams of this type include some natural gases, synthetic gases from coal and heavy oil gasification and tail gases from sulfur plants. Selectivity for H<sub>2</sub>S is needed either to enrich Claus sulfur plant feed in H<sub>2</sub>S or to remove only H<sub>2</sub>S when CO<sub>2</sub> removal is not necessary or economic. For the absorption of hydrogen sulfide into MDEA, the reaction which occurs can be considered to be instantaneous while carbon dioxide undergoes a second-order reaction with MDEA.

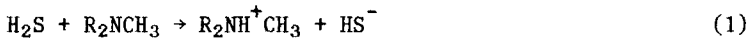
In this work, the simultaneous absorption of two gases into a liquid containing a reactant with which both gases react is modelled using the film theory. Physical properties and kinetic rate parameters used in the model have been measured in our laboratory. The model is used to study the effect of process variables on the selectivity of MDEA for H<sub>2</sub>S over CO<sub>2</sub>. The simultaneous absorption of H<sub>2</sub>S and CO<sub>2</sub> gases into aqueous MDEA is studied experimentally using a continuous stirred tank absorber. Experimental absorption rates are compared to predictions based on a multicomponent mass transfer model. The average deviations of the theoretical calculations from the experimental results are 10.2% and 12.9% for CO<sub>2</sub> and H<sub>2</sub>S, respectively.

INTRODUCTION

The objective of this work is to study the simultaneous absorption of  $\text{CO}_2$  and  $\text{H}_2\text{S}$  into aqueous methyldiethanolamine (MDEA) solutions. The simultaneous absorption of  $\text{CO}_2$  and  $\text{H}_2\text{S}$  into a solvent has a practical application in the purification of natural and refinery gases. Due to the need for energy conservation, attention has been directed recently towards using solvents that will selectively absorb  $\text{H}_2\text{S}$ . The tertiary amine used in this work, MDEA, has been found to be an effective solvent for the selective absorption of  $\text{H}_2\text{S}$  from a gas mixture containing  $\text{CO}_2$ .

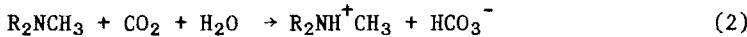
Tertiary amines such as MDEA react much faster with  $\text{H}_2\text{S}$  than with  $\text{CO}_2$ , resulting in selective absorption of  $\text{H}_2\text{S}$ . The use of MDEA to accomplish selective removal of  $\text{H}_2\text{S}$  was first reported by Frazier and Kohl (1) in 1950; however, commercial application of MDEA did not take place until the 1970's. Goar (2) points out the advantages of using MDEA compared to other amine solvents and describes several gas treating schemes employing MDEA. Daviet et al. (3) have reported improved performance of an amine gas treating plant when MDEA is substituted for diethanolamine. Simulation of amine treating units for simultaneous absorption of  $\text{H}_2\text{S}$  and  $\text{CO}_2$  has been carried out by Cornelissen (4), Tomcej et al. (5), and Sardar et al. (6,7,8).

When  $\text{H}_2\text{S}$  is absorbed into aqueous MDEA solution, it reacts with the amine to form the acid sulfide. The overall reaction is similar to the reaction of  $\text{H}_2\text{S}$  with other ethanolamine solutions such as monoethanolamine and diethanolamine. The reaction can be represented as



Since this reaction involves only the transfer of a proton, the kinetics will be very fast and the reaction may be modelled as being instantaneous.

The overall reaction between  $\text{CO}_2$  and MDEA is given by



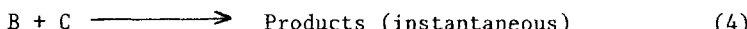
Several different mechanisms for this reaction have been proposed (4,9,10,11,12,13). In an earlier study we found that a mechanism similar to that proposed by Donaldson and Nguyen (14) for the reaction of  $\text{CO}_2$  with triethanolamine was consistent with our experiments on the kinetics of the reaction of  $\text{CO}_2$  and MDEA. In this mechanism, unprotonated MDEA is a base catalyst for hydration of  $\text{CO}_2$  to bicarbonate. According to Haimour et al. (12), the reaction between  $\text{CO}_2$  and MDEA is second order, first order with respect to the concentration of unprotonated MDEA, and first order with respect to concentration of  $\text{CO}_2$ . The second-order rate

constant reported by Haimour et al. (12) and used to interpret the absorption results reported here has the value 2.47 l/gmole s at 25° C. This value is lower than that found by Blauwhoff et al. (10), 4.8 l/gmole s, but is in agreement with that reported by Barth et al. (15), 3.2 ± 1.0 l/gmole s.

In this work the simultaneous absorption of H<sub>2</sub>S and CO<sub>2</sub> into aqueous MDEA solutions from a gas mixture with nitrogen as diluent was studied experimentally in a stirred cell absorption apparatus. The absorption rate data are compared to model predictions based on physicochemical properties. In addition, a film theory model is used to consider the effect of various process conditions on the selectivity of the solvent for hydrogen sulfide over carbon dioxide.

### THEORY

In this work, the film theory is used to model simultaneous gas absorption with chemical reaction in the liquid phase. Gas A (CO<sub>2</sub>) is assumed to react irreversibly with liquid reactant C (MDEA) under second-order conditions while gas B (H<sub>2</sub>S) undergoes an irreversible instantaneous reaction with C. The reaction system can be represented by



Since B and C react instantaneously, the liquid region where the reactions occur is divided into two distinct regions. Figure 1 illustrates the concentration profiles to be expected in these regions. Region I is characterized by the non-existence of C, Region II by the non-existence of B. Species B and C meet and react at  $x = x^*$ , where the concentration of both is zero.

In Region I, A and B diffuse without reaction and their concentration profiles can be described by the following steady-state diffusion equations in non-dimensional form:

$$\frac{d^2 a}{d\xi^2} = 0 \quad (5)$$

$$\frac{d^2 b}{d\xi^2} = 0 \quad (6)$$

where the non-dimensional variables are defined similar to Goettler and Pigford (16):

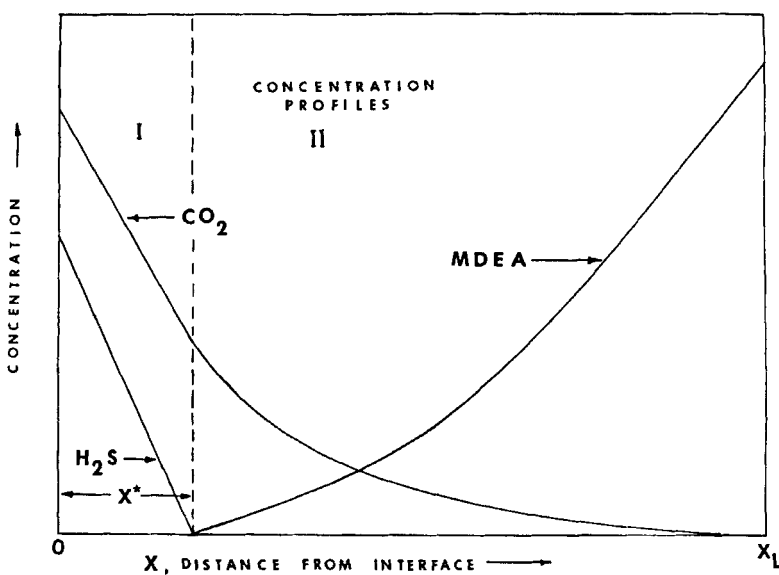


Fig. 1. Concentration Profile in the Liquid Showing Reaction Plane.

$$a = A/A_i \quad b = B/B_i \quad c = C/C_0 \quad \xi = x/x_L \quad (7)$$

The boundary conditions for Equations (5) and (6) are:

$$a(0) = 1 \quad b(0) = 1 \quad b(\xi^*) = 0 \quad (8)$$

The value of  $a$  at  $\xi = \xi^*$ , i.e.,  $a^*$ , is unknown; so an additional boundary condition is required to specify the system and couple the solution in Region I to that of Region II. This condition will be stated after the governing equations in Region II are presented.

In Region II, A and C undergo simultaneous diffusion and chemical reaction. Steady-state diffusion with second-order reaction is represented by

$$\frac{d^2 a}{d\xi^2} = M a c \quad (9)$$

$$\frac{d^2 c}{d\xi^2} = \frac{M m_A}{r_C} a c \quad (10)$$

where  $M = k_2 C_o D_A / k_{2A}^{02}$  (11)

and  $m_A = A_i / C_o$ ,  $r_C = D_C / D_A$  (12)

The boundary conditions for Equations (9) and (10) are:

$$c(\xi^*) = 0 \quad (13)$$

$$c(1) = 1 \quad (14)$$

$$a(\xi^*) = a^* \quad (15)$$

$$a(1) = 0 \quad (16)$$

The value of  $\xi^*$  and  $a^*$  are, however, unknown. An additional relationship relating Region I and Region II is obtained from the reaction stoichiometry between B and C. The rate at which C diffuses to  $\xi^*$  must be equal to the rate at which B diffuses toward  $\xi^*$ :

$$\frac{dc}{d\xi} = -m_B r \frac{db}{d\xi} \quad \text{at} \quad \xi = \xi^* \quad (17)$$

where

$$m_B = B_i / C_o \quad \text{and} \quad r = D_B / D_C \quad (18)$$

As shown by Goettler and Pigford (16) and Aiken (17), boundary condition (17) can be used to relate  $a^*$  and  $\xi^*$  by

$$a^* = 1 + \frac{m_B r r_C}{m_A} - \left( \frac{r_C + m_A + m_B r r_C}{m_A} \right) \xi^* \quad (19)$$

Therefore, either  $a^*$  or  $\xi^*$  can be chosen and integration can be carried out to match boundary condition (14). As pointed out by Aiken (17), this boundary value problem is inherently unstable integrating in either forward or backward direction. As suggested by Aiken (17), Gear's variable order predictor-corrector package was used in this work with a simple shooting method for the solution of the two-point boundary value problem.

The procedure used was to assume a value of  $\xi^*$  (usually a multiple of  $m_B$ ), calculate  $a^*$  from Equation (19), and solve the system of equations as an initial value problem. Values of  $\xi^*$  were subsequently corrected by the secant method to match condition (14). The local integration error was chosen to be  $10^{-5}$  and iterations were stopped when boundary condition (14) was met to within  $\pm 0.0001$ . Generally, less than 10 iterations were required for convergence in all runs.

The results are increasingly sensitive to the assumed values of  $\xi^*$  and  $a^*$  for large values of  $m_A$  and  $M$ , and the solutions become unstable for larger values of these parameters. An asymptotic analytical solution for large  $M$  is given by Goettler and Pigford (16) by assuming a linear concentration profile for  $C$

$$M^{1/3} = \frac{1.3717}{a^*} \frac{(1 - \xi^*)^{1/3}}{\xi^*} (1 - a^*) \quad (20)$$

The non-linear algebraic system of Equations (19) and (20) can be iteratively solved for  $a^*$  and  $\xi^*$ .

The enhancement factor is defined as the ratio of the rate of absorption with chemical reaction to that of purely physical absorption under the same hydrodynamic conditions. The rates of absorption with reaction are obtained from concentration gradients at the gas-liquid interface. In terms of dimensionless parameters, the enhancement factors are given by

$$E_A = - \frac{da}{d\xi} \Big|_{\xi=0} = \frac{1 - a^*}{\xi^*} \quad (21)$$

$$E_B = - \frac{db}{d\xi} \Big|_{\xi=0} = \frac{1}{\xi^*} \quad (22)$$

Selectivity,  $\sigma$ , is defined as the ratio of the enhancement factor for gas B over that of gas A,

$$\sigma = \frac{E_B}{E_A} = \frac{1}{1 - a^*} \quad (23)$$

This definition is appropriate as the hydrodynamics are assumed fixed and we wish to consider the effect of reaction on the absorption rate of B relative to A.

A typical computed concentration profile is shown in Figure 2. Figures 3 through 5 show the enhancement factor for gas B as a function of the diffusion-reaction parameter  $M$  with  $m_A$  and  $m_B$  as parameters. Figures 6 through 8 show the selectivity,  $\sigma$ , plotted as a function of  $M$  with  $m_A$  and  $m_B$  as parameters. The physico-chemical properties used in the calculations for Figures 3 through 8 correspond to absorption of hydrogen sulfide and carbon dioxide into 20 weight percent MDEA solution at 25°C. These properties were determined as discussed in the next section. The range of values of  $M$  used in the calculations covers the values likely to be encountered in industrial absorption columns.

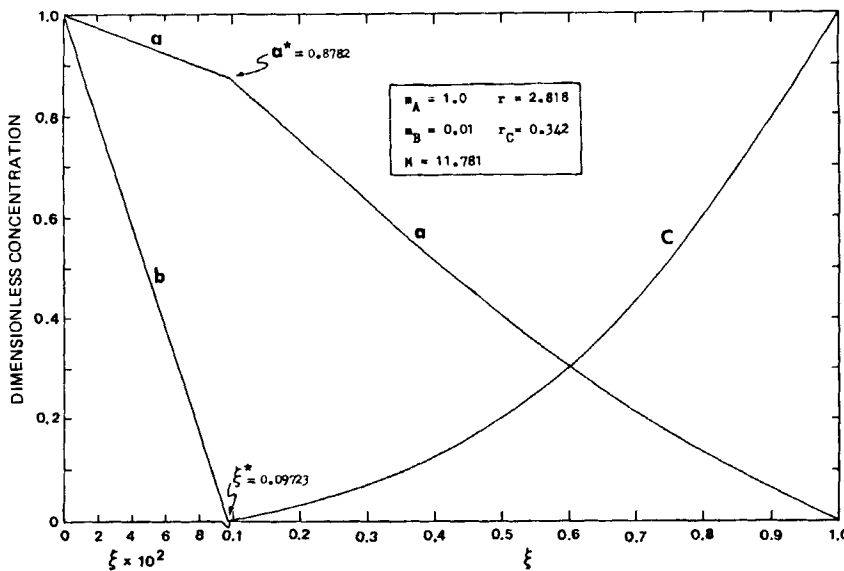
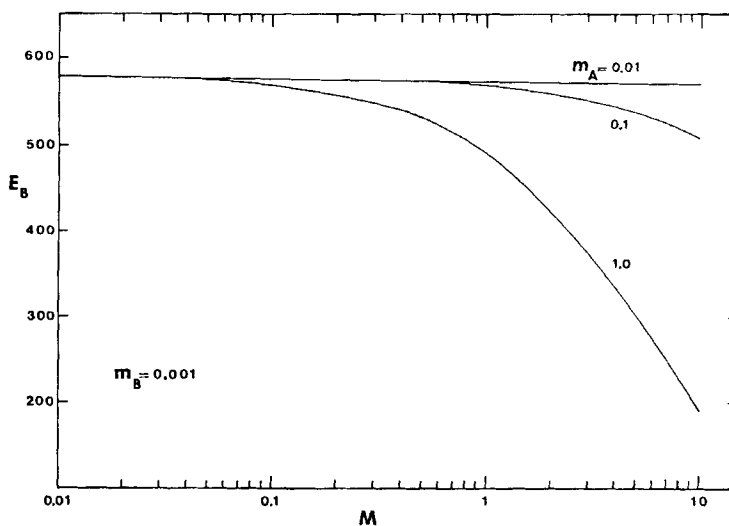


Fig. 2. Calculated Concentration Profiles in Liquid.

Fig. 3. Enhancement Factor for Gas B as a Function of M and  $m_A$  for  $m_B = 0.001$ .

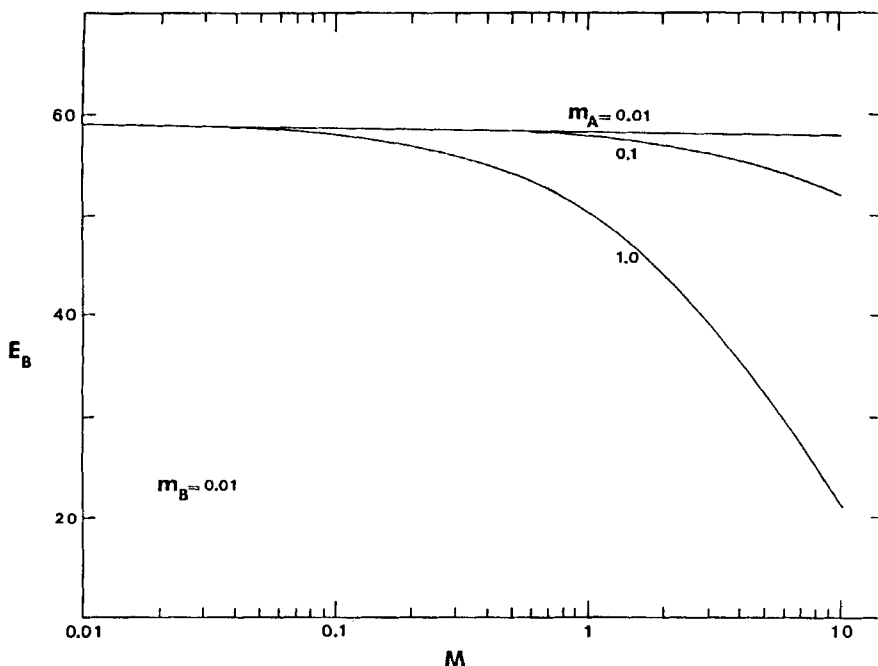


Fig. 4. Enhancement Factor for Gas B as a Function of M and  $m_A$  for  $m_B = 0.01$ .

It can be seen from Figures 3 through 8 that as  $m_A$  and  $m_B$  decrease, both  $E_A$  and  $E_B$  increase. However,  $E_A$  is less sensitive towards the change of  $m_A$  and  $m_B$  than  $E_B$ . The sensitivity of  $E_A$  and  $E_B$  towards the change of  $m_A$  and  $m_B$  increases with increasing M. Selectivity increases with decreasing M, and it changes rapidly at low M values. For lower M values,  $\sigma$  is very sensitive towards the change of  $m_B$  while it is less sensitive to the change of  $m_A$ .

To obtain high selectivity, it is preferred to have low values of  $m_A$  and  $m_B$ , which means low partial pressures of gases A and B or high concentration of amine. Also, absorbers with large physical mass transfer coefficients (short contact times) achieve higher selectivity since the value of parameter M is lowered. It is desirable to operate the absorber at lower temperatures, which leads to a lower value of the rate constant  $k_2$  and hence smaller M values. The effect of temperature on the selectivity of 20 wt % MDEA solution for hydrogen sulfide is shown in Figure 9. The physical properties and the reaction rate constant were obtained or

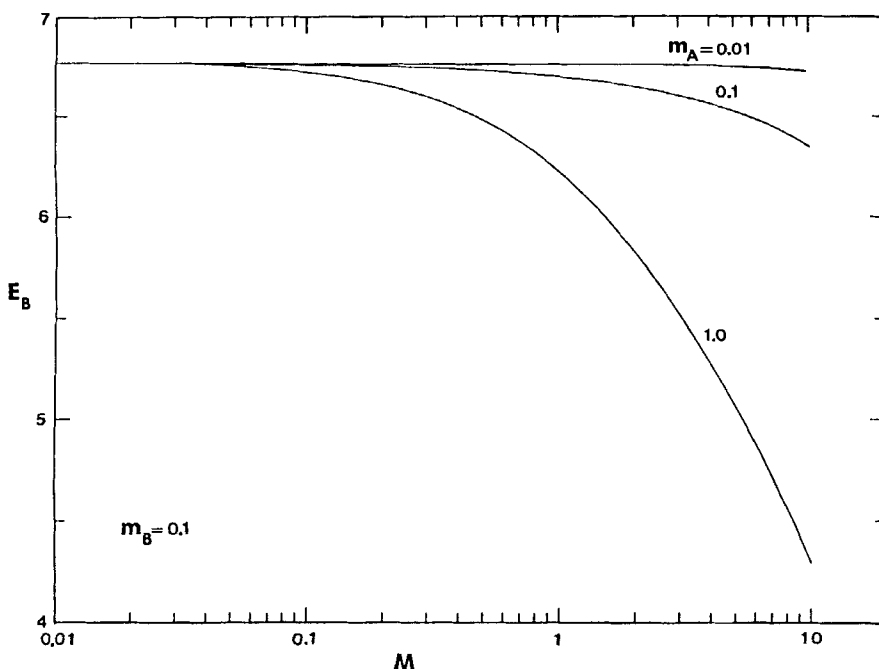


Fig. 5. Enhancement Factor for Gas B as a Function of  $M$  and  $m_A$  for  $m_B$  for  $m_B = 0.01$ .

extrapolated at each temperature from measurements made in our laboratory, as discussed in the following section of this work. It can be clearly seen that operating the absorber at lower temperatures leads to significantly higher selectivity.

The liquid reactant concentration  $C_o$  appears in the denominator of  $m_A$  and  $m_B$  but in the numerator of  $M$ . Therefore, increasing  $C_o$  would lead to a decrease in  $m_A$  and  $m_B$ , which is desirable from a selectivity viewpoint, but it also increases the value of  $M$  which has the effect of lowering selectivity. The net effect of increasing  $C_o$  was observed to be an increase in selectivity. This result is due to the higher sensitivity of the selectivity to  $m_B$  than to  $M$ , at least in the parameter range of this study. Therefore, for higher selectivity, a higher liquid reactant concentration is warranted.

Summarizing the results of the model predictions, higher selectivity for hydrogen sulfide is obtained in absorbers having short contact times, operating at low temperatures and using

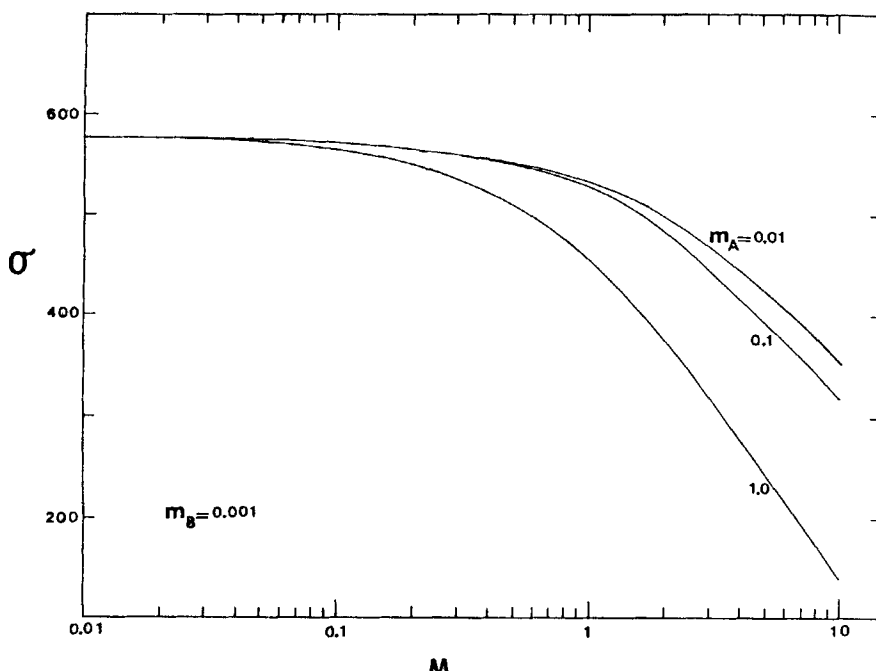


Fig. 6. Selectivity as a Function of  $M$  and  $m_A$  for  $m_B = 0.001$ .

concentrated amine solutions. Also, low partial pressures of  $\text{CO}_2$  and  $\text{H}_2\text{S}$  in the absorber would lead to higher selectivity. Therefore, it is desirable to operate the absorber at lower pressures from a selectivity point of view.

As mentioned in the Introduction, we have experimentally studied the simultaneous absorption of  $\text{H}_2\text{S}$  and  $\text{CO}_2$  into aqueous MDEA solutions in a stirred-cell absorber. A general model, taking into account mass transfer resistances in both gas and liquid phases, is used here to predict absorption rates for hydrogen sulfide and carbon dioxide into the MDEA solutions. Since the number of components in either phase exceeds two, a multicomponent transport model has to be used to describe the overall resistance offered by the two-phase system. For  $n$ -component systems, the transport behavior in either phase is adequately described by a matrix of transport coefficients with  $(n-1)^2$  elements (Stewart and Prober, (18)). The proper formulation for addition of phase resistances in multicomponent systems is given by Krishna (19):

$$[K_{oyb}^*]^{-1}[\beta_b^y]^{-1} = [k_{yb}^*]^{-1}[\beta_b^y]^{-1} + [M][k_{xb}^*]^{-1}[\beta_b^x]^{-1} \quad (24)$$

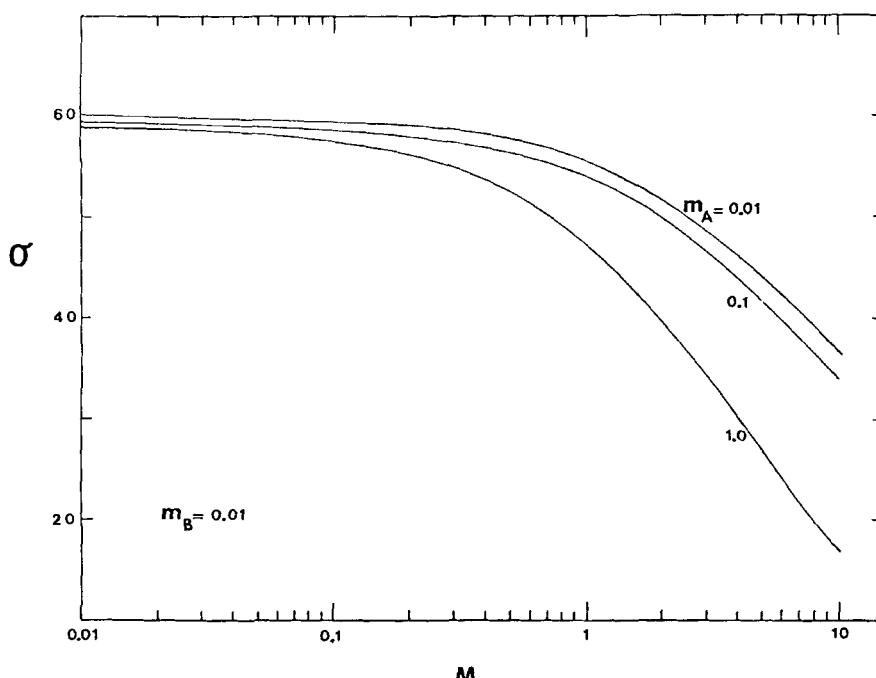


Fig. 7. Selectivity as a Function of  $M$  and  $m_A$  for  $m_B = 0.01$ .

The superscript black dot  $\cdot$  indicates that these coefficients are themselves dependent on the interfacial mass transfer rates. The subscript  $b$  refers to bulk fluid conditions. The matrix  $[M]$  is a matrix of equilibrium 'constants' with elements

$$M_{ij} = \frac{\partial y_i^*}{\partial x_j} \quad i, j = 1, 2, \dots, n-1 \quad (25)$$

This matrix will, in general, be non-diagonal for non-ideal system. For this gas absorption process, both phases can be considered ideal and the matrix  $[M]$  reduces to a diagonal matrix with elements given by

$$M_{11} = \frac{H_{CO_2}^* C}{P} \quad (26)$$

$$M_{22} = \frac{H_{H_2S}^* C}{P} \quad (27)$$

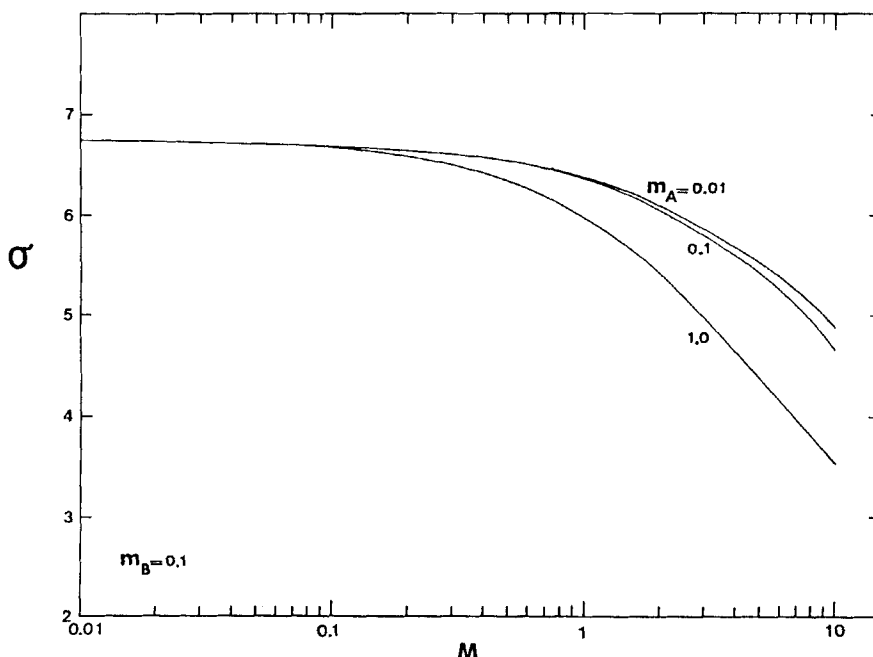


Fig. 8. Selectivity as a Function of  $M$  and  $m_A$  for  $m_B = 0.1$ .

The matrices  $[\beta_b^y]$  and  $[\beta_b^x]$  are "bootstrap solution" matrices which allow the calculation of total fluxes  $N_i$  from diffusion fluxes  $J_{bi}$ :

$$(N) = [\beta_b^y] (J_b^y) = [\beta_b^x] (J_b^x) \quad (28)$$

The bootstrap solution matrix for the absorption case has its elements given by (Krishna, 19):

$$\beta_{bij}^y = \delta_{ij} + y_{ib}/y_{nb} \quad , \quad i, j = 1, 2, \dots, n-1 \quad (29)$$

where the subscript  $n$  refers to the stagnant component, nitrogen. In the liquid phase,  $[\beta_b^x]$  essentially reduces to the identity matrix

$$[\beta_b^x] = [I] \quad (30)$$

since the concentration of the diffusing species 1 and 2 are small.

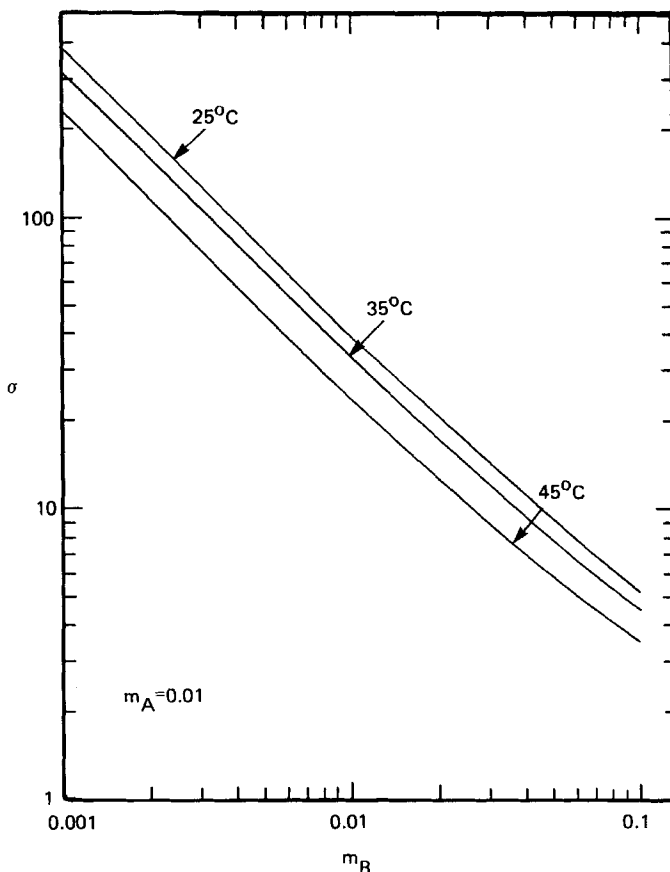


Fig. 9. Effect of Temperature on Selectivity.

The elements of the zero-flux gas phase mass transfer coefficient matrix  $[k_{yb}]$  for a ternary system are given by Krishna (20) in terms of the constituent binary coefficients  $k_{ij}$ :

$$k_{yb_{11}} = k_{13} (y_{1b} k_{23} + (1-y_{1b}) k_{12})/S \quad (31)$$

$$k_{yb_{12}} = y_{1b} k_{23} (k_{13} - k_{12})/S \quad (32)$$

$$k_{yb_{21}} = y_{2b} k_{13} (k_{23} - k_{12})/S \quad (33)$$

$$k_{yb_{22}} = k_{23} (y_{2b} k_{13} + (1-y_{2b}) k_{12})/S \quad (34)$$

where  $S$  is given by

$$S = y_{1b} k_{23} + y_{2b} k_{13} + y_{3b} k_{12} \quad (35)$$

The finite-flux matrix  $[k_{yb}]$  is obtained from

$$[k_{yb}] = [k_{yb}] [E] \quad (36)$$

where  $[E]$  is a correction factor matrix that accounts for the effect of high mass transfer rates on the mass transfer coefficients. For transfer of two species through a third stagnant component, i.e.,  $N_3 = 0$ , the elements of  $[E]$  are given by Krishna and Standart (21):

$$E_{11} = (\hat{E}_1 \phi_{12} + \hat{E}_2 \phi_{21}) / (\hat{\phi}_1 - \hat{\phi}_2) \quad (37)$$

$$E_{12} = (\hat{E}_1 - \hat{E}_2) \phi_{12} / (\hat{\phi}_1 - \hat{\phi}_2) \quad (38)$$

$$E_{21} = (\hat{E}_1 - \hat{E}_2) \phi_{21} / (\hat{\phi}_1 - \hat{\phi}_2) \quad (39)$$

$$E_{22} = (\hat{E}_1 \phi_{21} + \hat{E}_2 \phi_{12}) / (\hat{\phi}_1 - \hat{\phi}_2) \quad (40)$$

where  $\hat{\phi}_1 = N_1/k_{13} + N_2/k_{23}$  (41)

$$\hat{\phi}_2 = (N_1 + N_2)/k_{12} \quad (42)$$

$$\hat{E}_1 = \frac{\hat{\phi}_1}{\exp \hat{\phi}_1 - 1} \quad (43)$$

$$\hat{E}_2 = \frac{\hat{\phi}_2}{\exp \hat{\phi}_2 - 1} \quad (44)$$

$$\phi_{12} = -N_1 (1/k_{12} - 1/k_{13}) \quad (45)$$

$$\phi_{21} = -N_2 (1/k_{12} - 1/k_{23}) \quad (46)$$

In the liquid phase, the correction factor matrix  $[E]$  can be taken to be the identity matrix. In addition, each gas can be assumed to diffuse independently of the other and there are no diffusional interactions to give rise to non-zero off-diagonal elements. Therefore,  $[k_{xb}]$  becomes a diagonal matrix with elements given by

$$\dot{k}_{xb_{11}} = k_{\ell A}^o C E_A \quad (47)$$

$$\dot{k}_{xb_{22}} = k_{\ell B}^o C E_B \quad (48)$$

The film theory model previously described is used to calculate the enhancement factors E<sub>A</sub> and E<sub>B</sub>. Comparison of the simple asymptotic result by Goettler and Pigford (16) with the exact numerical solution of the film theory model showed a maximum error of only about 1.5% in E<sub>A</sub> and 0.3% in E<sub>B</sub> for M values as low as 10. For the experimental conditions used in this work, the lowest value of parameter M is about 12; m<sub>A</sub> and m<sub>B</sub> are smaller than about 0.005. Therefore, it was decided to use the above asymptotic solution to calculate E<sub>A</sub> and E<sub>B</sub> for considerable reduction in computation time and little loss of accuracy.

An iterative solution is needed to compute the fluxes N<sub>i</sub>. Initial values for compositions of CO<sub>2</sub> and H<sub>2</sub>S at the gas-liquid interface are assumed. The individual phase mass transfer coefficients are computed and combined to obtain an overall gas phase mass transfer coefficient matrix [K<sub>yb</sub><sup>ovb</sup>]. The fluxes J<sub>i</sub> and N<sub>i</sub> are then computed and the compositions at the interface are calculated and used to restart the computations. Convergence is obtained when the assumed and calculated compositions are equal. At each iteration, the iterative algorithm of Krishna and Standart (21) is used to compute the correction factor matrix [E] and [k<sub>yb</sub>].

#### PHYSICAL PROPERTIES

The physicochemical properties needed to model the simultaneous absorption rates of CO<sub>2</sub> and H<sub>2</sub>S are the diffusion coefficient for both gases in the liquid, the solubilities of both gases in the liquids, the diffusion coefficient for MDEA in solution and the kinetics of the reaction between CO<sub>2</sub> and MDEA. Haimour et al. (12) have studied the kinetics of this reaction over the temperature range 15-35°C. As mentioned in the Introduction, we have experimentally determined the second-order rate constant for the reaction between CO<sub>2</sub> and MDEA at 25°C to be

$$k_2 = 2.47 \text{ } \ell/\text{gmole s} \quad (49)$$

The diffusivity of CO<sub>2</sub> into aqueous MDEA solutions was determined experimentally by Haimour and Sandall (22) using the N<sub>2</sub> analogy method. The data may be correlated by

$$\frac{D_{CO_2} \mu^{0.54}}{T} = 6.109 \times 10^{-8} \quad (50)$$

Equation (50) fits the data to within an absolute mean deviation of 2.3% for data collected over the temperature range 15 to 35°C and for MDEA concentrations up to 20 wt%. The liquid viscosity needed to implement Equation (50) was correlated by a modified form of the equation proposed by Lobe (23).

$$\mu = \phi_A \mu_A e^{\phi_B \alpha_B^*} + \phi_B \mu_B e^{\phi_A \alpha_A^*} \quad (51)$$

where  $\alpha_A^* = -1.7 \ln \mu_B / \mu_A$  (52)

$$\alpha_B^* = 0.39 \ln \mu_B / \mu_A + (2.70 \ln \mu_B / \mu_A)^{1/2} \quad (53)$$

The viscosity of pure MDEA,  $\mu_B$ , needed for Equation (51) can be fitted over the temperature range 20 to 80°C by

$$\mu_B = 1.378 \times 10^{-5} \exp \left( \frac{4,622}{T} \right) \quad (54)$$

The viscosity data fit Equations (51) and (54) to within absolute mean deviations of 1.5% and 4.5%, respectively.

The solubility of CO<sub>2</sub> in aqueous MDEA solutions was also obtained using the N<sub>2</sub>O analogy method by Haimour and Sandall (22). The data were obtained over the temperature range 15 to 35°C and for amine concentrations up to 40 wt%. The data can be fitted to within an absolute mean deviation of 1.5% by

$$\ln H_{CO_2} = A - \frac{B}{T} \quad (55)$$

where  $A = 12.212 - 0.4815 C_{MDEA} - 0.04666 C_{MDEA}^2$  (56)

$$B = 2,627.3 - 158.76 C_{MDEA} - 15.612 C_{MDEA}^2 \quad (57)$$

The diffusivity of H<sub>2</sub>S in aqueous MDEA solutions was obtained by correcting its value in pure water for the effect of the viscosity of the solution according to the relation

$$\frac{D_{H_2S} \mu}{T}^{0.74} = 5.836 \times 10^{-8} \quad (58)$$

This correlation was obtained experimentally by Haimour and Sandall (24) for the diffusivity of H<sub>2</sub>S in water at different temperatures.

The solubility of H<sub>2</sub>S in the amine solutions was obtained by correcting the values in pure water for the salting-out effect of different ions presented in the solution using the Van Krevelen and Hoftijzer relation (25), i.e.

$$\log(H/H^\circ) = hI \quad (59)$$

where  $I$  is the ionic strength of the solutions and is defined by:

$$I = \frac{1}{2} \sum C_i Z_i^2 \quad (60)$$

$h$  is the sum of contributions of different species in the solution, i.e.

$$h = h_+ + h_- + h_G \quad (61)$$

During the simultaneous absorption of H<sub>2</sub>S and CO<sub>2</sub> into the amine solution, an instantaneous reaction regime is formed near the gas liquid interface as a result of the reaction between H<sub>2</sub>S and the amine. In this regime, R<sub>2</sub>NH<sup>+</sup>CH<sub>3</sub> and SH<sup>-</sup> ions are present. The salting out parameter for R<sub>2</sub>NH<sup>+</sup>CH<sub>3</sub> is not known, but it may be assumed to be zero. This assumption was used by Hikita et al. (26,27,28) for the analysis of CO<sub>2</sub>-aqueous MEA, CO<sub>2</sub>-aqueous NH<sub>3</sub>, and CO<sub>2</sub>-aqueous DEA systems, respectively. The value of the salting-out parameter for SH<sup>-</sup> can be assumed to have a similar value to that of OH<sup>-</sup>, i.e. 0.066 l/g ion (29). The salting-out parameter for H<sub>2</sub>S gas is -0.033 l/g mole (29).

The diffusivity of MDEA in solution has been measured experimentally by Haimour and Sandall (30). At 25°C the diffusivities were found to be 0.83x10<sup>-5</sup> cm<sup>2</sup>/s and 0.60x10<sup>-5</sup> cm<sup>2</sup>/s for 10 and 20 wt% solutions of MDEA.

#### EXPERIMENTAL APPARATUS AND PROCEDURE

A drawing of the stirred cell absorber used in the work is shown in Figure 10. The absorber is 10 cm in diameter and is 30 cm long. The gas-liquid contact area is 78.3 cm<sup>2</sup>. The absorber has two independent impellers for the gas and liquid phases. Both impellers are centered on one shaft and are 7.6 cm in diameter. The gas impeller shaft is a hollow tube and the liquid impeller shaft passes through it. Mercury seals are provided between the two shafts and also between the outer shaft and the top flange. The maximum speed for the liquid stirrer is limited to 135 rpm by the requirement of keeping a smooth gas-liquid interface. The cell temperature is kept constant by circulating an aqueous ethylene glycol solution through a jacket surrounding the absorber. The absorber has four baffles to reduce vortex formation. Each baffle is made from 0.64 cm diameter tubing and extends from the bottom of the absorber to above the gas-liquid interface.

Figure 11 shows a schematic drawing of the complete absorption apparatus. Pure MDEA was diluted with freshly boiled deionized water to give the desired amine concentration. The amine solution was pumped to an overflow weir above the reactor in order to dampen any flow rate oscillations. The solution flow rate was measured by

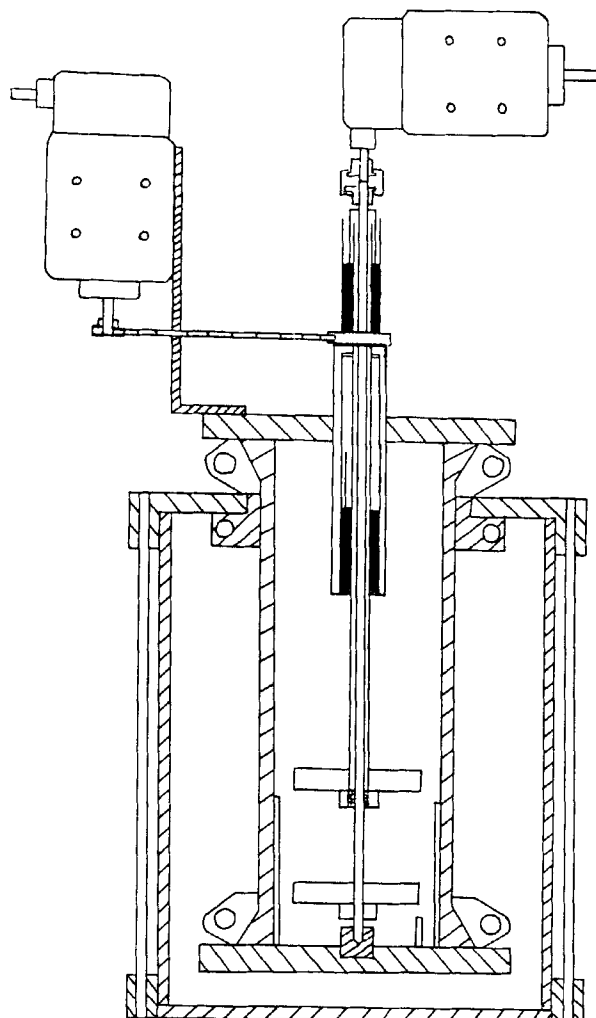


Fig. 10. Stirred Cell Absorber.

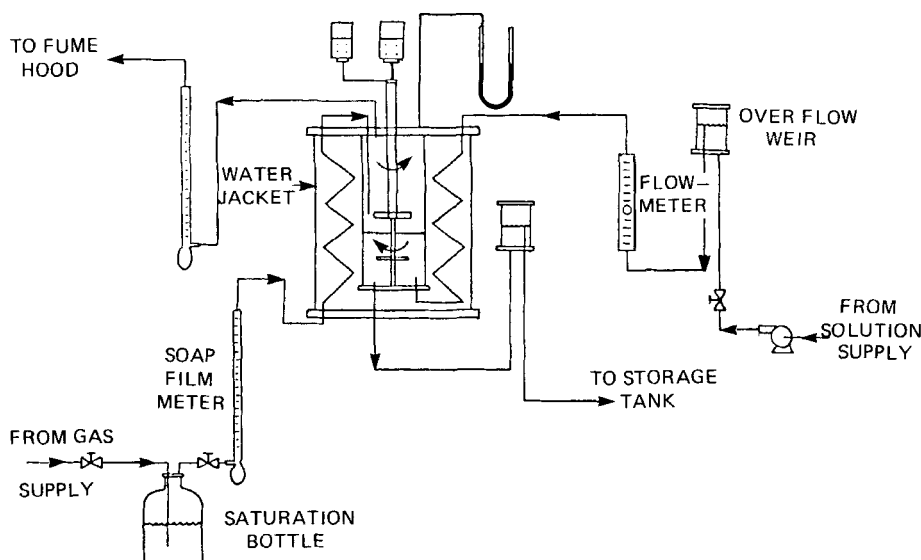


Fig. 11. Schematic Drawing of Experimental Apparatus.

a calibrated rotameter and then passed through a coil in the water jacket surrounding the reactor. The solution was introduced to the reactor from the bottom and distributed by a 0.60 cm diameter perforated tube which extends about 3 cm from the bottom. The liquid flow rate was about  $110 \text{ cm}^3/\text{min}$  during all experiments. The volume of solution inside the reactor was about  $500 \text{ cm}^3$ . The level of solution inside the reactor was kept constant by continuous drawing of solution through another overflow weir.

The gases used were  $N_2$ ,  $CO_2$  and  $H_2S$  having purities of 99.99%, 99.8% and 99.5%, respectively. For the simultaneous absorption experiments, each gas passed through a high pressure regulator followed by a low pressure regulator and was saturated with water in a sparger. Gas flow rates in and out of the reactor were measured by soap film meters. Exit gas concentrations were measured using a gas chromatograph.

## RESULTS AND DISCUSSION

### A. Liquid Phase Mass Transfer Coefficient, $k_L^0$ :

The liquid phase mass transfer coefficient for physical absorption was measured experimentally by Haimour et al. (12) by

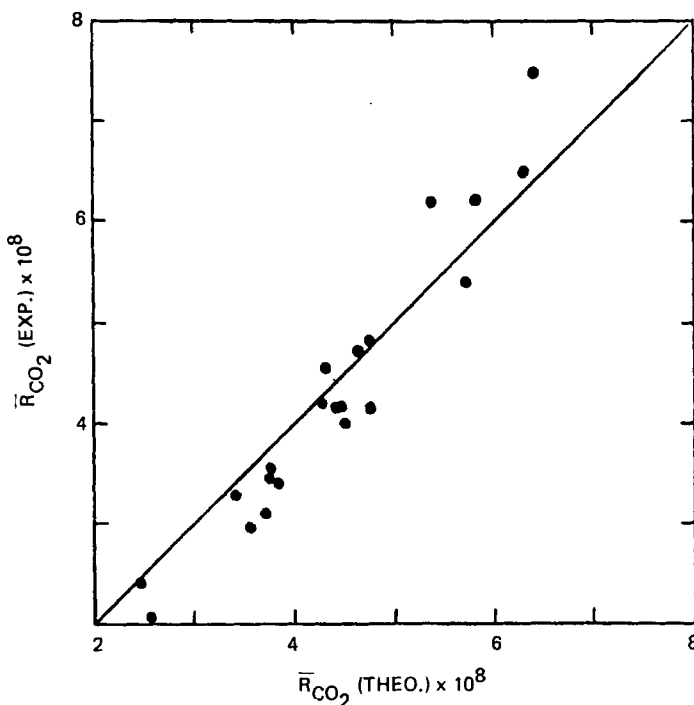


Fig. 12. Experimental Absorption Rate of  $CO_2$  Compared to Predicted Absorption Rate.

absorbing  $N_2O$  into 10 wt% and 20 wt% aqueous MDEA solutions at 25°C. The data were correlated as

$$Sh_\ell = 0.0977 Re_\ell^{0.66} Sc^{\frac{1}{2}}, \quad 2 \times 10^3 < Re_\ell < 1 \times 10^4 \quad (62)$$

#### B. Gas Phase Mass Transfer Coefficient, $k_y$ :

The binary gas phase mass transfer coefficient was measured by absorbing  $H_2S$  diluted with  $N_2$  into 10 wt% and 20 wt% aqueous MDEA solutions at 25°C. The partial pressure of  $H_2S$  gas was varied from 0.080 to 0.137 atm. Under these conditions, the mass transfer is completely gas phase controlled. The criteria for gas phase control is

$$k_{g,H_2S} p_{H_2S} < k_{\ell,H_2S}^0 \sqrt{D_{MDEA}/D_{H_2S}} C_0 \quad (63)$$

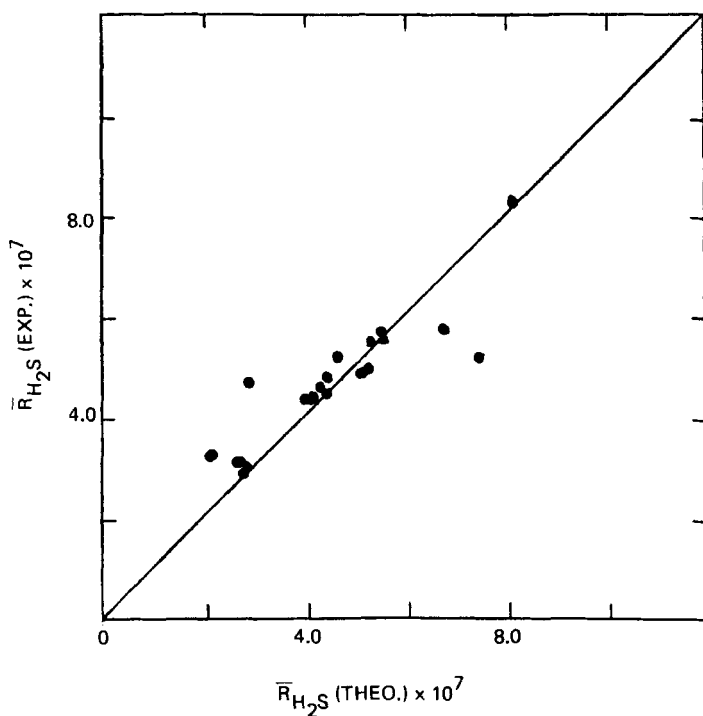


Fig. 13. Experimental Absorption Rate of  $\text{H}_2\text{S}$  Compared to Predicted Absorption Rate.

The value of  $k$  was found to be  $5.30 \times 10^6$  g moles/cm<sup>2</sup>s atm for the 10 wt% MDEA solution and  $6.29 \times 10^6$  g moles/cm<sup>2</sup>s atm for the 20 wt% MDEA solution. The gas phase impeller was positioned closer to the interface for the 20% MDEA experiments, thus accounting for the higher mass transfer coefficient.

#### C. Simultaneous Absorption of $\text{CO}_2$ and $\text{H}_2\text{S}$ :

Simultaneous absorption of  $\text{H}_2\text{S}$  and  $\text{CO}_2$  into aqueous MDEA solutions from a gas mixture with nitrogen as diluent was studied at 25°C. The partial pressure of  $\text{CO}_2$  was varied from 0.14 to 0.41 atm while that of  $\text{H}_2\text{S}$  varied from 0.03 to 0.12 atm. The speed of the liquid stirrer was varied from 56 to 115 rpm. The rates of absorption of  $\text{CO}_2$  and  $\text{H}_2\text{S}$  were calculated from the difference between the inlet and outlet flowrates of each gas.

The binary gas phase mass transfer coefficients  $k_{ij}$  were calculated from the measured value of  $k_g$  by assuming a  $2/3$  power dependence of  $k_{ij}$  on the binary diffusivity, as suggested by the boundary layer theory. The measured  $k_g$  values were corrected for the effect of high mass transfer rates by applying a film theory correction.

From the analysis of the data, it was found that the composition of  $H_2S$  at the interface is essentially zero for all runs indicating that the absorption of  $H_2S$  is entirely gas phase controlled. The rate of absorption of  $CO_2$  was not affected by gas phase resistance. The reaction of  $CO_2$  with the amine is under pseudo-first order reaction conditions and the rate of absorption is given by Danckwerts (29)

$$\tilde{R}_A = k_{LA}^0 A_i \sqrt{1 + M} \quad (64)$$

The rate of absorption of  $H_2S$ , however, is somewhat affected by the presence of  $CO_2$  in the gas phase as indicated by nonzero cross coefficients in the matrices  $[k_{ij}]$  and  $[K_{ij}]$ . Figures 12 and 13 show plots of calculated versus experimentally measured absorption rates. The average deviation of the theoretical model from the experimental results is 10.2% and 12.9% for  $CO_2$  and  $H_2S$ , respectively.

Under these conditions, the selectivity for  $H_2S$  absorption depends mainly on the gas phase resistance. This model may be used for the lean end of industrial absorbers where  $H_2S$  absorption is controlled by gas phase resistance. To increase the selectivity for  $H_2S$  absorption, the gas phase resistance has to be lowered to the range where the liquid phase resistance for  $H_2S$  absorption becomes significant and has to be included in the analysis.

#### ACKNOWLEDGMENTS

We gratefully acknowledge the support of this research by the National Science Foundation through NSF Grant No. CPE-8315809. The MDEA used in this work was donated by the Union Carbide Company. Noman Haimour received a fellowship from the University of Jordan, Amman, Jordan.

#### NOMENCLATURE

a dimensionless concentration of gas A

a\* dimensionless concentration of gas A at the reaction plane

A	constant defined in Equation (56)
A	concentration of gas A, gmole/l
$A_i$	interfacial concentration of gas A, gmole/l
b	dimensionless concentration of gas B
B	constant defined in Equation (57)
$B_i$	interfacial concentration of gas B, gmole/l
c	dimensionless concentration of liquid reactant C
C	total molar concentration in liquid, g mole/l
$C_i$	molar concentration of ionic species i in liquid, gmole/l
$C_{MDEA}$	concentration of MDEA in aqueous solution, gmole/l
$C_o$	concentration of MDEA in the bulk liquid, gmole/l
d	impeller diameter, cm
D	diffusivity, $cm^2/s$
E	enhancement factor
[E]	matrix of correction factors
H	Henry's law constant, $l atm/gmole$
h	solubility factor, $l/gmole$
[I]	identity matrix
$J_i$	molar diffusion flux of species i, $gmole/cm^2s$
$k_2$	second-order rate constant $l/gmole s$
$k_{\ell}^o$	physical absorption mass transfer coefficient, $cm/s$
$k_{\ell}^{\cdot}$	chemical absorption mass transfer coefficient, $cm/s$
$k_{ij}$	constituent binary pair gas phase mass transfer coefficients, $gmole/cm^2s atm$
[ $k^{\cdot}$ ]	partial matrix of multicomponent mass transfer coefficients
[ $K_o^{\cdot}$ ]	overall matrix of multicomponent mass transfer coefficients

$\ell$	absorber diameter, cm
[M]	matrix of equilibrium constants
M	dimensionless parameter = $k_2 C_o D_A / k_\ell^o A^2$
$m_A$	concentration ratio = $A_i / C_o$
$m_B$	concentration ratio = $B_i / C_o$
n	number of species in mixture
$N_\ell$	speed of liquid impeller, rps
$N_i$	total molar flux of species i, gmole/cm <sup>2</sup> s
P	total pressure, atm
$\bar{R}$	rate of absorption, gmole/cm <sup>2</sup> s
r	diffusivity ratio = $D_B / D_C$
$r_C$	diffusivity ratio = $D_C / D_A$
$Re_\ell$	Reynolds number = $d^2 N_\ell \rho / \mu$
S	variable defined in Equation (35)
Sc	Schmidt number = $\mu / \rho D$
Sh	Sherwood number = $k_\ell^o \ell / D$
T	temperature, °K
$x_i$	mole fraction of species i in the liquid phase
$x_L$	film thickness, cm
$y_i$	mole fraction of species i in the gas phase
Z	valence of ionic species

#### Greek Symbols

$\alpha_A^*$	constant defined by Equation (52)
$\alpha_B^*$	constant defined by Equation (53)
[ $\beta$ ]	bootstrap solution matrix
$\delta_{ij}$	Kronecker delta
$\mu$	viscosity of aqueous MDEA solution, cP

$\mu_A$	viscosity of pure water, cp
$\mu_B$	viscosity of pure MDEA, cp
$\phi_A$	volume fraction of water in solution
$\phi_B$	volume fraction of MDEA in solution
$\rho$	density of solution, g/cm <sup>3</sup>
$\sigma$	selectivity for gas B = $E_B/E_A$
$\xi$	dimensionless distance into the liquid
$\xi^*$	dimensionless distance to reaction plane

Matrix

( )	column matrix of dimension <u>n-1</u>
[ ]	square matrix of dimension, <u>n-1</u> x <u>n-1</u>
[ ] <sup>-1</sup>	inverted matrix, <u>n-1</u> x <u>n-1</u>

Subscripts

b	bulk phase property
y	gas phase property
x	liquid phase property
A	property corresponding to $CO_2$
B	property corresponding to $H_2S$
C	property corresponding to MDEA
G	property corresponding to dissolved gas
l	liquid phase property
+	property corresponding to cations in solution
-	property corresponding to anions in solution

Superscripts

*	equilibrium value
•	coefficient corresponding to finite mass transfer rates
o	property corresponding to water

REFERENCES

1. Frazier, H.D., and A.L. Kohl, *Ind. Eng. Chem.*, 42, 2288 (1950).
2. Goar, B.G., *Oil and Gas J.*, 78, 239 (1980).
3. Daviet, G.R., R. Sundermann, S.T. Donnelly, and J.A. Bullin, *Hydrocarbon Processing*, p. 79, May (1984).
4. Cornelissen, A.E., *Trans. I. Chem. E.*, 58, 242 (1980).
5. Tomcej, R.A., F.D. Otto and F.W. Nolte, paper presented at the Gas Conditioning Conference, Norman, Oklahoma (1983).
6. Sardar, H., M.S. Sivasubramanian and R.H. Weiland, paper no. 87c, presented at the AIChE Houston meeting, March (1985).
7. Sivasubramanian, M.S., H. Sardar and R.H. Weiland, paper no. 87e, presented at the AIChE Houston meeting, March (1985).
8. Sardar, H., M.S. Sivasubramanian and R.H. Weiland, paper presented at the Gas Conditioning Conference, Norman Oklahoma (1985).
9. Barth, D., Tondre, C., Lappal, G., and J.-J. Delpuech, *J. Phys. Chem.*, 85, 3660 (1981).
10. Blauwhoff, P.M.M., G.G. Versteeg, and W.P.H. Van Swaaij, *Chem. Eng. Sci.*, 38, 1411 (1983).
11. Danckwerts, P.V., *Chem. Eng. Sci.*, 34, 443 (1979).
12. Haimour, N., A. Bidarian and O.C. Sandall, paper submitted to *Chem. Eng. Sci.* (1986).
13. Yu, W.-C., G. Astarita and D.W. Savage, *Chem. Eng. Sci.*, 40, 1585 (1985).
14. Donaldson, T.L., and Y.N. Nguyen, *I&EC Fund.*, 19, 260 (1980).
15. Barth, D., C. Tondre, and J.-J. Delpuech, *Chem. Eng. Sci.*, 39, 1753 (1984).
16. Goettler, L.A. and R.L. Pigford, *AIChE J.*, 17, 793 (1971).
17. Aiken, R.C., *Chem. Eng. Sci.*, 37, 1031 (1982).
18. Stewart, W.E., and R. Prober, *Ind. Eng. Chem. Fundamentals*, 3, 224 (1964).

19. Krishna, R., Letters in Heat and Mass Transfer, 3, 41 (1976).
20. Krishna, R., Chem. Eng. Sci., 32, 659 (1977).
21. Krishna, R. and G.L. Standart, AIChE J., 22 (1976).
22. Haimour, N., and O.C. Sandall, Chem. Eng. Sci., 39, 1791 (1984).
23. Lobe, V.M., M.S. Thesis, University of Rochester, Rochester, NY (1973).
24. Haimour, N., and O.C. Sandall, J. Chem. Eng. Data, 29, 20 (1984).
25. Van Krevelen, D.W. and P.J. Hofstijzer, Chim. Ind. Numero Speciale du XXI<sup>e</sup> Congress International de Chimie Industrielle (Bruxelles), 168 (1948).
26. Hikita, H., S. Asai, H. Ishikawa, and K. Uku, Chem. Eng. Commun. 5, 315 (1980).
27. Hikita, H., S. Asai, and Y. Hinukashi, Kagaku Kogaku, 35, 1021 (1971).
28. Hikita, H., S. Asai, S., Y. Katsu, and S. Ikuno, J. Chem. Eng. Data, 25, 324 (1980).
29. Danckwerts, P.V., "Gas-Liquid Reactions", McGraw-Hill Book Co., New York, NY, (1970).
30. Haimour, N. and O.C. Sandall, paper submitted to Chem. Eng. Sci. (1985).